

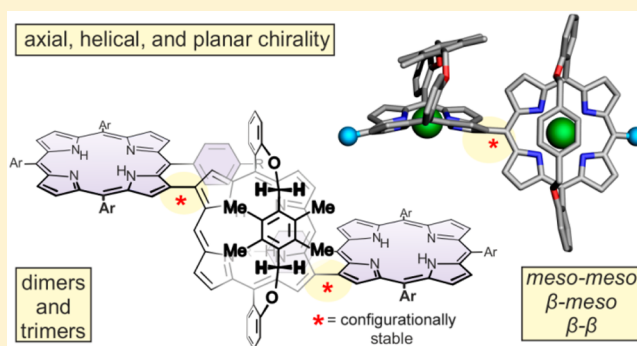
Axial, Helical, and Planar Chirality in Directly Linked Basket-Handle Porphyrin Arrays

Andreas C. Gehrold, Torsten Bruhn,* and Gerhard Bringmann*

Institute of Organic Chemistry, University of Würzburg, Am Hubland, D-97074 Würzburg, Germany

Supporting Information

ABSTRACT: The single-electron oxidative dimerization of basket-handle porphyrins (BHPs) with different coordinated metal ions [Cu(II), Ni(II), Pd(II), Zn(II)] yielded directly *meso-meso* linked dimers in excellent yields. The synthetic protocol is suited for coupling substrates with different *meso*-substituents (H, Br, aryl, alkyl) opposite to the coupling site. Experimental findings concerning reactivities and selectivities were in good agreement with theoretical investigations using ALIE calculations. The dimers, which all are axially chiral, were resolved into their enantiomers by HPLC on a chiral phase. ECD spectra were measured in the stopped-flow mode and compared with results from quantum-chemical ECD calculations to assign the absolute configuration. One directly linked dimer was further oxidized to a fused system, which possessed a stable helical chirality. Its absolute configuration was again assigned by ECD investigations. Furthermore, functionalized BHPs and tetraarylporphyrins were coupled under Suzuki conditions to give dimers and trimers with either β -*meso* or β - β linkages. Because of the steric shielding of one of the BHP hemispheres, the products were formed with full diastereoselectivity regarding all porphyrin-porphyrin axes. The stereostructures of these arrays were investigated by quantum-chemical calculations (DFT-D3, TD DFT, and sTD DFT), and the absolute configurations were assigned for all chiral representatives.



INTRODUCTION

Among the various topics of tetrapyrrole chemistry, conjugated porphyrin arrays have always attracted broad interest due to the interaction of multiple chromophores.^{1,2} More recently, the field of directly fused porphyrins was opened with the synthesis of mono, doubly, and triply linked representatives with variations of the coupling position between *meso-meso*, *meso- β* , and β - β , which yielded a plethora of multiporphyrin systems.^{1,3,4} Synthetically, directly linked and fused bisporphyrins can be prepared by oxidative dimerization with Ag(I) salts,⁵ BAHA,⁶ DDQ-Sc(OTf)₃,⁷ AuCl₃-AgOTf,⁸ and PIFA^{9,10} or electrochemically¹¹ by Ullmann homocoupling,¹² Suzuki coupling,^{13,14} or dimerization of radicals derived from Senge-type reactions with lithium organyls.^{15,16}

Although various directly linked or fused porphyrin dimers are known, chiral representatives are rare and often their absolute stereostructure is not fully known. This is mainly due to the inherent high symmetry of the D_{4h}-symmetric porphyrin core, which complicates the synthetic access and stereochemical analysis of unsymmetric compounds. The intensively studied *meso-meso* coupled dimers are achiral as long as the *meso* substituents orthogonal to the axis are identical.^{5,8,10,12,15-17} Nonidentical substituents lead to the loss of all mirror planes within the dimer and therefore to an unsymmetric and thus axially chiral structure (Figure 1A). We have discovered several examples of such *meso-meso* linked systems in the literature,

where, however, the axial chirality was not recognized at all, and only one case where enantiomers had been resolved but absolute configurations were not assigned.¹⁸⁻²⁴ The same chirality criteria apply for β -*meso* linked bisporphyrins: If the *meso*-coupled building block comprises two identical *meso* substituents orthogonal to the axis, the resulting bisporphyrin is achiral.²⁵ In all cases with nonidentical *meso* substituents, the resulting structure is chiral (Figure 1B). The β - β dimers, by contrast, are intrinsically chiral independent of their substitution pattern (Figure 1C).¹⁴ *Meso-meso*, β - β doubly linked dimers are helically chiral due to the steric hindrance of the remaining opposing β -protons (Figure 1D).²⁶ For all chiral examples from Figure 1, the enantiomers were resolved, and their ECD spectra were reported.^{14,24,26} Although several *meso-meso* linked porphyrin dimers were described in the literature, their axial chirality has rarely been recognized¹⁸⁻²⁴ but rather often overlooked, and to the best of our knowledge, until now, no absolute configuration of such chiral systems has been elucidated. In the case of β -*meso* and β - β dimers, the absolute stereostructures were assigned by comparison of their experimental ECD spectra with the calculated ones.^{13,14,27} The absolute configuration of the doubly linked dimer was initially assigned by a wrong application of the exciton chirality

Received: November 18, 2015

Published: January 5, 2016

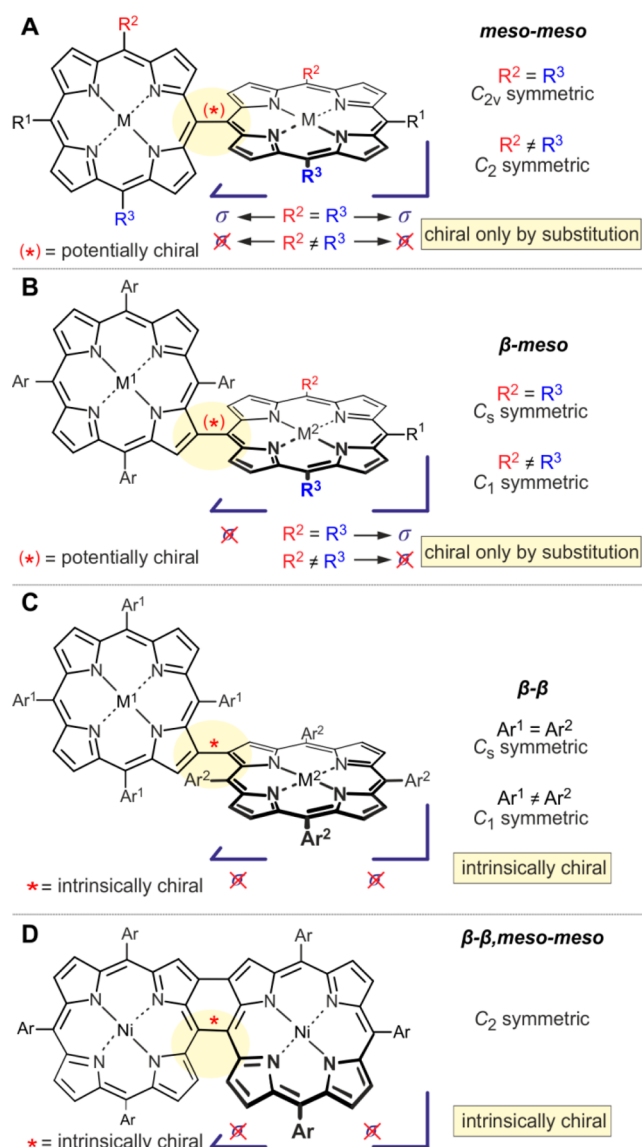


Figure 1. Origin of chirality in directly linked and in fused porphyrin dimers.

method²⁸ and has later been revised²⁶ by using quantum-chemical ECD calculations. This example nicely demonstrates the difficulties and snares with the stereostructural elucidation of compounds consisting of multiple chromophores with electronic/excitonic interactions.²⁹

We describe here the synthesis of di- and trimeric porphyrin arrays with diverse coupling motifs and different types of chirality. Our approach makes use of the special stereostructure of basket-handle porphyrins (BHPs), which allows the differentiation between the two hemispheres of the tetrapyrrolic macrocycle. This reduces their symmetry, and the steric shielding caused by the handle enables diastereoselective coupling reactions between the porphyrin building blocks. Although BHPs have been known for a long time, they still are objects of very recent research.^{30–34} Thus, it was surprising to not find even a single example of a directly linked or fused BHP, regardless of the linkage position, capping type or porphyrinoidic structure. The work described here closes this gap and aims to demonstrate the potential of BHPs in the

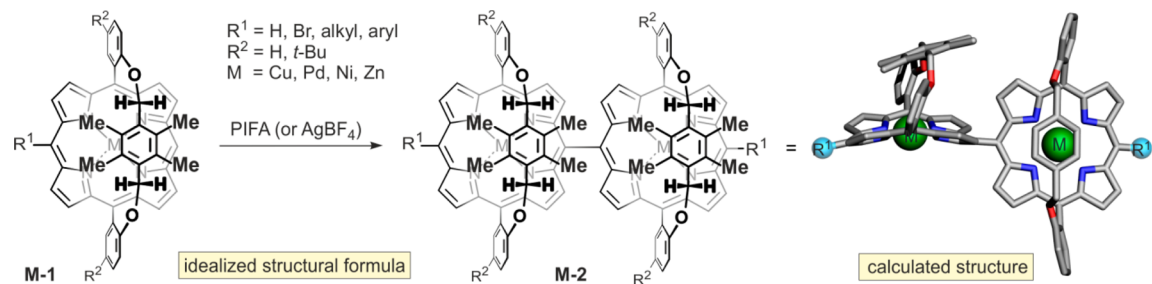
(diastereoselective) construction of porphyrin arrays and their intriguing chiral features.

RESULTS AND DISCUSSION

Synthesis of Directly *meso-meso* Linked BHPs by Oxidative Coupling. The simplicity, reliability, and wide applicability of one-electron oxidative coupling reactions in the synthesis of directly linked porphyrin dimers^{8–10,35,36} prompted us to investigate such protocols in the synthesis of dimeric *meso-meso* linked BHPs. [Bis(trifluoroacetoxy)iido]benzene (PIFA) as well as Ag(I) salts proved to convert the monomeric BHPs M-1²⁵ to the corresponding *meso-meso* dimers M-2 in excellent yields within short reaction times (Table 1).

These reaction conditions were successfully applied to 5,10,15-triaryl-type metallo-BHPs with Ni(II), Cu(II), or Pd(II) as complexed metals, and the dimers were isolated in almost quantitative yields. By contrast, the Zn(II) dimer could initially not be isolated and only decomposition products were detected. The peculiarities of the Zn(II) BHPs regarding their reactivity and stability will be discussed later. Furthermore, it was shown for a series of Ni(II)-BHPs that this method can be used to dimerize substrates with aryl, alkyl, halogen, or no substituents opposite to the coupling site. As known and expected from literature results¹⁰ in the case of Ni-1a with two free *meso* positions, the reaction gave a mixture of oligomerization products. Ni-1a was reacted with 0.6 equiv of PIFA, and the product mixture was purified by preparative recycling gel permeation chromatography. Along with 16% of recovered starting material and 22% of the dimer, 18% of the trimer, 8% of the tetramer, and 15% of a mixture of higher oligomers were isolated. Oligomers larger than the dimer were characterized only by mass spectrometry and not further investigated as all attempts to resolve the diastereomers or even the enantiomers failed. The 2-fold *meso*-unsubstituted dimer Ni-2a was also prepared in an overall yield of 90% in a directed, two-step procedure by dimerizing the brominated BHP Ni-1d and reducing the dimer Ni-2d using the previously reported hydrodebromination protocol with Pd(PPh₃)₄ as a catalyst and formic acid as a hydrogen source.⁸ Efforts to dimerize In(III)-BHPs were not successful, as only starting material was recovered after a prolonged reaction time even at elevated temperature and when using strong oxidants. The MALDI-MS investigations of the reaction of Mg(II)-BHPs with PIFA or AgBF₄ indicated the formation of dimeric species that were partially demetalated. The resulting free-base BHP dimers rapidly decomposed during the reaction or at the latest during workup; thus, no dimers were isolated from this reaction. Consequently, further attempts to obtain a free-base dimer did not seem promising.

Astonishingly, the monomeric Zn(II) BHPs decompose in solutions open to oxygen within 24 h. Other Zn(II) porphyrins are stable to air and moisture,^{37,38} but already a simple amino substituent in the β -position of a Zn(II) porphyrin is known to lead to a similar instability.²⁷ Under argon atmosphere and in solid state, the Zn(II) BHPs were stable even if exposed to light and humidity. MALDI-MS experiments hinted at an oxidative degradation, because regardless of the reaction and workup conditions prior to the measurement, peaks with M+16 and M+32 were detected, which seemed to correspond to the uptake of one or two oxygen atoms. During the dimerization reaction of Zn(II) BHPs, even with substoichiometric amounts of oxidant, thin layer chromatography for reaction monitoring only indicated the presence of remaining starting material and

Table 1. Synthesis of Directly *meso-meso* Linked Basket-Handle Porphyrins^a


entry	monomer M-1	metal	R ¹	R ²	dimer M-2	time (min) ^b	yield (%)
1	Ni-1a	Ni	H	<i>t</i> -Bu	Ni-2a	5	22
2	Ni-1b	Ni	<i>n</i> -Bu	H	Ni-2b	2	97
3	Ni-1c	Ni	(4- <i>t</i> -Bu)Ph	H	Ni-2c	5	98
4	Ni-1d	Ni	Br	<i>t</i> -Bu	Ni-2d	60	96
5	Pd-1e	Pd	(4- <i>t</i> -Bu)Ph	<i>t</i> -Bu	Pd-2e	5	97
6	Zn-1f	Zn	<i>n</i> -Hex	H	Zn-2f	5	26
7	Cu-1c	Cu	(4- <i>t</i> -Bu)Ph	H	Cu-2c	5	99

^aReaction of M-1 (1.0 μ M) in dichloroethane under an argon atmosphere; 0.6 equiv PIFA; M-2 synthesized as a racemic mixture. ^bTime until no starting material was detectable by TLC.

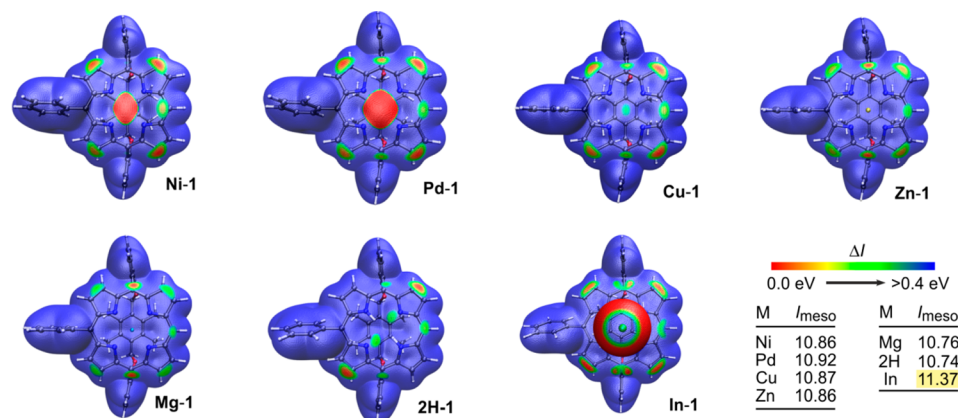
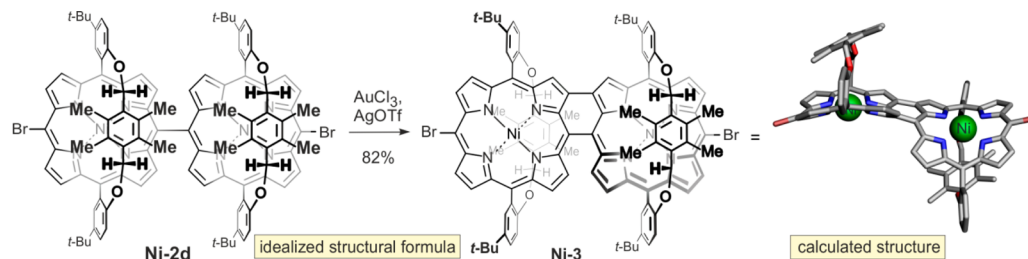


Figure 2. ALIE surfaces of different BHP monomers **1**; the regioselectivities for an electrophilic attack are similar in all cases. The absolute values of *I* in the *meso* position show that the nucleophilicity in **In-1** is significantly lower, thus making a reaction unlikely in this case.

Scheme 1. Synthesis of *meso-meso*, β - β Doubly Linked Basket-Handle Porphyrin^a

^aSynthesized as a racemic mixture.

highly polar decomposition products. Regardless of the workup protocol, no dimeric products were isolated. After assessing various reaction conditions without success, parameters of reactivity were evaluated by average localized ionization energy (ALIE) calculations³⁹ to investigate whether the experimental findings were a problem of reactivity or selectivity, or whether they were due to the rapid decomposition of initially formed product. We have recently shown how ALIEs can help rationalizing the oxidative coupling reaction of porphyrins.²⁷ Assuming the same reaction mechanisms in this case, the ALIE

calculations clearly showed that the electronic situations in the Zn(II) and Mg(II) BHPs were very similar to those of the Ni(II), Cu(II), and Pd(II) BHPs regarding their reactivity and selectivity, as they showed similar ALIE surfaces with only slightly different absolute average localized ionization energies (Figure 2). The only exception was the In(III) BHP, which had significantly larger energy values (*I*) and thus can most probably not react as a nucleophile in the oxidative coupling. The ALIE investigations hinted at problems with the stability of the Zn(II) dimers. The BHP **Zn-1f** was then reacted with a

slight excess of oxidant for a prolonged time under argon to ensure full conversion of the monomer, and the reaction mixture was quickly filtered over a short plug of silica. Immediate removal of the solvent under reduced pressure finally yielded the dimer **Zn-2f** in 26% yield and sufficient purity for NMR characterization. We tested the stability of the dimer in solution open to air and found full decomposition within a few minutes. All efforts to resolve the enantiomers by HPLC on a chiral phase thus failed due to the instability of the dimer.

Synthesis and Stereostructure of a Doubly Linked Dimer. To investigate if our BHP dimers can be reacted with the same selectivity to yield either helically chiral (doubly linked) or planar (triplly fused) systems like the *meso-meso* dimers previously reported by Osuka's group, we applied the $\text{AuCl}_3\text{-AgOTf}$ -mediated oxidation conditions to dimer **Ni-2d**. In contrast to the reported control between doubly and triply linked bisporphyrins by variation of the reagent concentration, only one product was formed in good yield (Scheme 1).

Under conditions described to preferentially yield the doubly linked product (1 equiv AuCl_3 , 6 equiv AgOTf), only **Ni-3** was formed exclusively in 82% yield. Triply linked dimers or the stereoisomer with both handles on the same side of the bisporphyrin plane were not detected. The same results were found with conditions usually providing triply linked dimers in excellent yields (2 equiv AuCl_3 , 10 equiv AgOTf). This can be explained by the geometry of the monomeric BHPs and the resulting structure of the *meso-meso* dimers. In the case of the BHPs described here, the tetrapyrrole core is highly bent due to the shortness of the bridging strap. During the oxidation of the *meso-meso* dimer **Ni-2d**, the first linkage occurred at the β -position in a way that diastereoselectively only the *anti*-bridge product was formed, most likely caused by steric effects. This was a dead end with respect to the formation of the triply linked product because the remaining two β -positions are too distant to allow further reaction. Efforts to couple the monomer **Ni-1d** directly to the β -*meso*, β -*meso* fused dimer with $\text{AuCl}_3\text{-AgOTf}$ as described in the literature⁸ were not successful.

Photophysical Properties and Stereostructural Elucidation of the Dimeric BHPs. Directly linked porphyrins have been shown to possess interesting absorption properties^{6,13,14,27} due to the interaction between the two porphyrin chromophores and due to the overall change in the chromophore in fused systems. The UV/vis spectra of the *meso-meso* linked and the fused BHP dimers (Figure 3) are very similar to those of previously reported structures with an identical porphyrin linkage but without the handle.⁸ The *meso-meso* linked dimers showed a broadened and split Soret band but were otherwise not significantly different from their monomers. The doubly linked dimer had a UV spectrum nearly identical to the one of the unbridged example described in the literature.⁸ This means that even the high degree of distortion in the tetrapyrrole caused by the shortness of the strap has only minor effects on the photophysical properties of the chromophore even in dimeric systems.

In view of the chiral nature of the *meso-meso* linked and of the fused dimeric BHPs, elucidation of the absolute configuration of these chiral dimers seemed rewarding. Except for the **Zn(II)** dimer **Zn-2f** (because of its chemical instability), all dimers were resolved by HPLC on a chiral phase, and their online ECD spectra were measured in the stopped-flow mode. The experimental spectra were compared with the ones derived from quantum-chemical ECD calculations to assign the

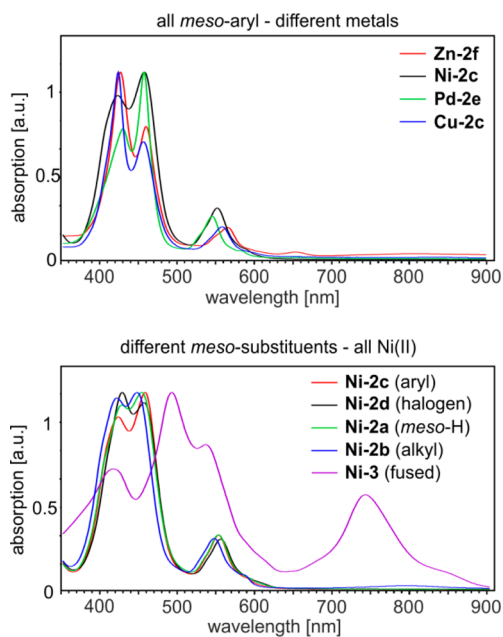
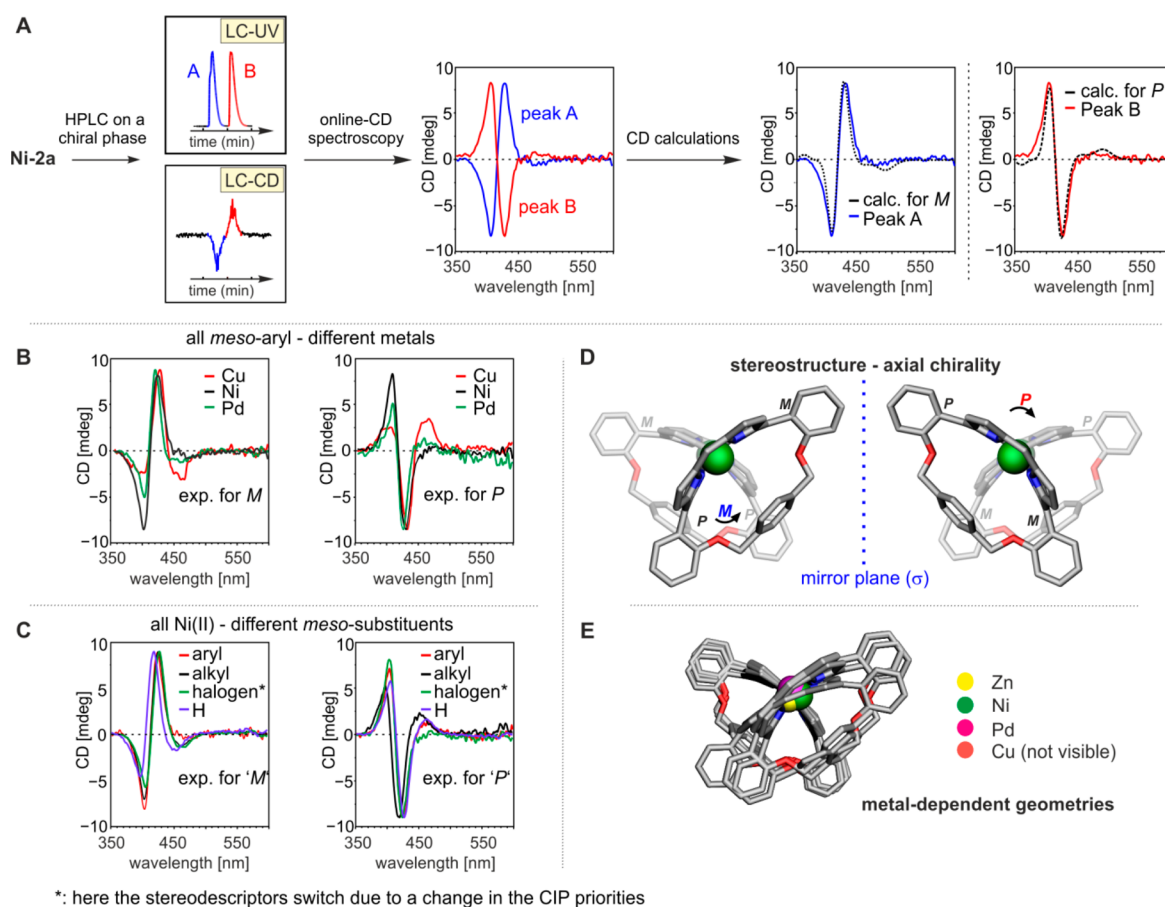


Figure 3. UV/vis spectra of directly linked BHPs **M-2** and of a fused one (**Ni-3**).

absolute configuration. Previous findings had proven that TD CAM-B3LYP calculations were well-suited to predict the ECD spectra of porphyrins and porphyrin dimers.^{25,27,40} However, this full TD approach is very time-consuming; thus, the simplified TD DFT (sTD DFT) approach of Grimme et al. was evaluated for the dimers investigated in this paper. As already described by the Grimme group, e.g., for a bacteriochlorin dimer,⁴¹ the sTD DFT results were, also in the case of the porphyrin dimers described herein, even better than the full TD ones using only a fraction of the computational time. In the following, only the results of the best-matching sTD calculations are shown (sTD CAM-B3LYP/def2-SVP or sTD B3LYP/def2-SVP), whereas the results of the other calculations can be found in the Supporting Information.

For the *meso-meso* dimer **Ni-2c**, which will be discussed exemplarily for all *meso-meso* dimers, the ECD spectrum showed a couplet around 415 nm (Figure 4A), which corresponds to the absorption of the Soret band (Figure 3). The spectra of peaks A and B were fully mirror imaged to each other, which is evidence of the presence of enantiomers, with Peak A showing a positive couplet and Peak B a negative one around 415 nm. Conformational analysis of **Ni-2a** gave only one relevant conformation with the porphyrin planes being nearly orthogonal to each other (Figure 4D). The sTD B3LYP ECD spectra calculated for **Ni-2a** with the *M*-configuration at the central (i.e., porphyrin-porphyrin) axis fit very well to the ECD curve of the faster eluting enantiomer (Peak A), which thus was assigned the *P,M,M,M,P*-configuration. Because of the symmetry of the structure, the descriptors of the outer axes (between the porphyrin and the handle-bearing aryl group) were essential to determine the descriptor of the central axis. However, the monomeric BHP units are identical and each of them has a mirror plane; thus, only the central axis is decisive, and there are only two enantiomers *P,M,M,M,P* (which is the same as *M,P,M,P,M*) and *P,M,P,M,P* (which is the same as *M,P,P,P,M*).⁴² Without the rotational hindrance at the central axis, the compound would be *meso*. In the following, we will thus only discuss the descriptor of the central axis. As a result,



*: here the stereodescriptors switch due to a change in the CIP priorities

Figure 4. (A) Resolution and determination of the absolute configurations of *meso-meso* linked Ni-2a by HPLC-ECD in combination with quantum-chemical ECD calculations (sTD B3LYP/def2-SVP). Comparison of the experimental ECD spectra of (B) differently metalated BHP dimers and (C) differently substituted Ni-BHP dimers for the elucidation of the absolute configurations of these compounds. (D, E) B97-D3/def2-TZVP optimized structures of M-2 with different central metals.

all *meso-meso* coupled BHPs M-2 with a positive couplet are *M*-configured, whereas those with a negative couplet possess *P* configuration (for the brominated compound Ni-2d, the stereodescriptors differ due to a change in the CIP priorities). Determination of the absolute configurations by using the exciton chirality rule gave identical results. The Soret band of the monomer consists of two excitations: one with a transition dipole moment (TDM) parallel to the bridge and one orthogonal to it (both in the porphyrin plane). In the dimer, the TDMs orthogonal to the bridge are linearly aligned and thus give no exciton couplet, whereas the other ones do. According to the orientation of these TDMs in the optimized structures (Figure 4D), the *M*-configured dimer M-Ni-2a thus has a positive exciton couplet, and *P*-Ni-2a has a negative one. The structure of Ni-2a is C_2 -symmetric and thus the rules for a degenerated system had been applied.

Comparison of the ECD spectra of the Ni(II), Cu(II), and Pd(II) BHP dimers showed only minor differences in the relative intensities of the peaks, whereas the spectra were qualitatively very similar (Figure 4B). This was in agreement with the calculated minimum structures that likewise showed very similar geometries (Figure 4E). The same was true for the series of Ni(II) BHP Ni-2a-d dimers with different *meso* substituents opposite the coupling site (Figure 4C).

The reports on the elucidation of the absolute configuration of the β - β , *meso-meso* fused dimeric Ni(II) porphyrin, described in the Introduction (Figure 1D), have included UV and ECD

spectra^{26,26} that are very similar to the ones we measured for the doubly fused BHP Ni-3. As the strap in the BHPs did not have a significant effect on the UV and ECD spectra, the absolute helical configuration of Ni-3 was simply determined by comparison of the experimental ECD curves with that reported by Osuka from TD B3LYP calculations.²⁶ However, we additionally performed quantum-chemical ECD calculations to assess the suitability of different density functionals (B3LYP, B3LYP, and CAM-B3LYP in comparison to CC2 results). Not surprisingly, the B3LYP functional performed worse in predicting the UV curve of Ni-3, and CAM-B3LYP provided much better results (Figure 5 and Supporting Information). The unexpected good fit of the ECD curves calculated with TD B3LYP can only be explained by error compensation effects. Like those described above for the *meso-meso* dimers, sTD gave even superior fits of experimental and calculated ECD spectra ($\Delta_{\text{ESI}}^{43} = 90\%$ for sTD CAM-B3LYP, $\Delta_{\text{ESI}} = 76\%$ for TD CAM-B3LYP) as compared to those achieved by the full TD approach. The only exception was sTD B3LYP ($\Delta_{\text{ESI}} = 57\%$), which is worse than the full TD B3LYP ($\Delta_{\text{ESI}} = 87\%$) results; thus, obviously, no error compensation took place here.

Synthesis of β -*meso* Linked Porphyrin Dimers and Trimers by Suzuki Coupling of Functionalized BHPs. The synthesis of directly linked porphyrin arrays comprising different monomeric subunits and varying coupling sites usually requires an approach via transition metal-catalyzed cross-coupling reactions of suitably functionalized building blocks

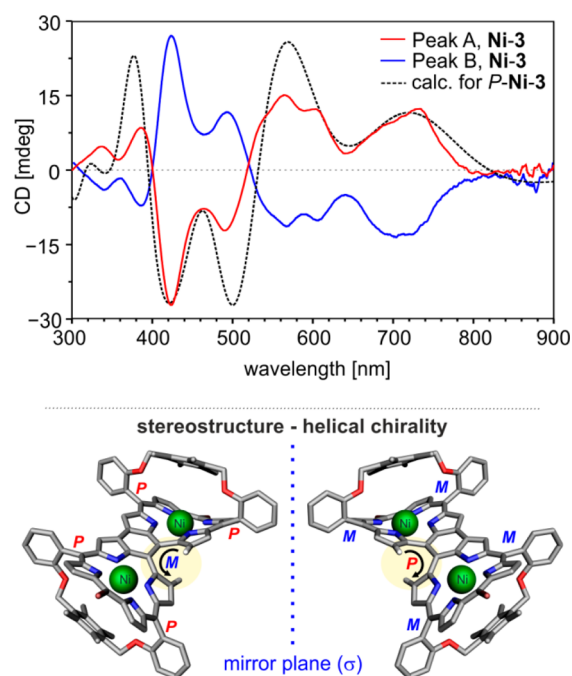


Figure 5. Experimental and calculated (sTD CAM-B3LYP/def2-SVP) ECD spectra and absolute configurations of *meso-meso*, β - β fused BHPs.

because oxidative coupling reactions of porphyrins are limited to only the most reactive position. Recent reports^{1,13,14} on the Suzuki coupling of porphyrins had proven the broad scope and reliability of this synthetic route for the formation of either direct β -*meso* or β - β bonds between two porphyrin units. We have recently extended this approach to BHPs and described two first examples of directly linked bisporphyrins bearing BHP subunits.²⁵

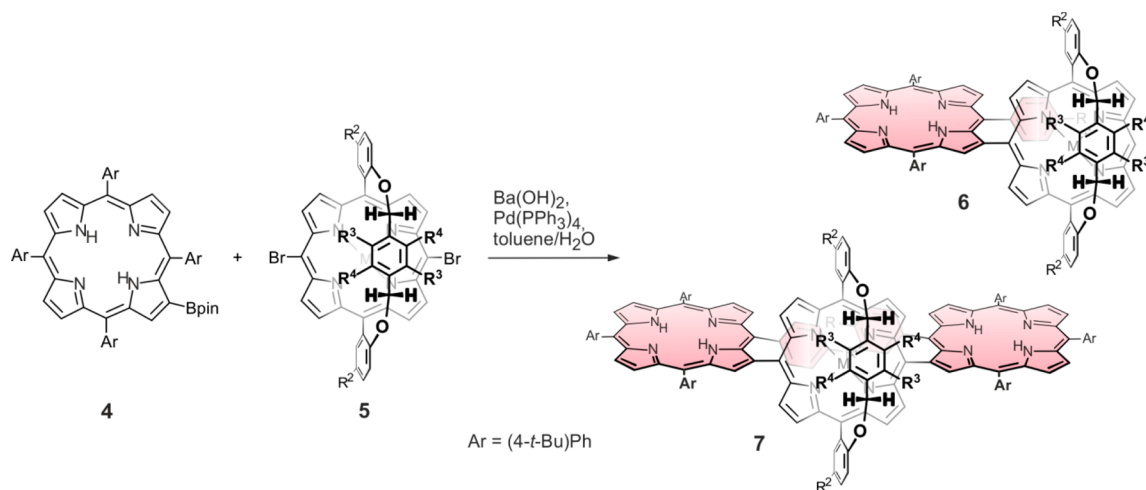
Analogously, the protocol was used for the synthesis of β -*meso* coupled trimers (Table 2). Reaction of the β -borylated

tetraarylporphyrin **4** with the *meso*-dibrominated BHP **5** yielded the β -*meso* coupled trimer **7** in good yield along with dimer **6**, which is a side product formed by hydrodebromination that occurred during the reaction.

Previous syntheses of β -*meso* linked porphyrin trimers with tetraarylporphyrins as the “outer” units had always yielded a mixture of *cis* and *trans* isomers regarding the aryl units adjacent to the axis.¹³ The use of a BHP as the central building block seemed promising to prevent the formation of the *trans* trimer and thus to permit the directed diastereoselective synthesis of *cis* trimers. This was our initial motivation to start investigations on BHPs, and indeed, the steric shielding of one of the BHPs hemispheres completely prohibited the formation of the *trans* isomer. Both the dimers **6** and the trimers **7** were found to adopt a conformation with the *meso*-aryl substituent of the tetraarylporphyrins located on the sterically unhindered side of the BHP. Previous *cis* trimers had shown an unprecedented chirality that originated from chiral conformations as a result of the hindered exchange of the aryl-rings at the central porphyrin.¹³ However, in case of trimer **7a**, VT NMR investigations (see Supporting Information) showed that these conformations are even less stable than those of the compounds described earlier.

Stereostructural Elucidation of β -*meso* Linked Porphyrin Dimers and Trimers. The β -*meso* coupled arrays **6** and **7** were achiral in those cases where they had been synthesized from the achiral BHP **5a**. However, if the dibrominated BHP building block possessed an unsymmetric xylene⁴⁴ unit, i.e., $R^3 \neq R^4$, and was thus planar-chiral itself, the dimers, as well as the trimers, became chiral too. As all reactions were carried out with either achiral or racemic material, and no chiral information was introduced during the Suzuki coupling, all products were formed as racemic mixtures. The enantiomers of the chiral dimers and trimers were resolved by HPLC on a chiral phase, and their ECD spectra were measured online by LC-CD in the stopped-flow mode. During the measurements, severe difficulties occurred, and it was initially not possible to

Table 2. Suzuki Coupling of β -Borylated Tetraarylporphyrins **4** with *meso*-Brominated BHPs **5**



entry	S	R ²	R ³ /R ⁴	M	6, yield (%)	7, yield (%)
1	5a	H	Me/Me	2H	6a, 32	7a, 60
2	5b	<i>t</i> -Oct ^a	H/Me	2H	6b, 30 ^b	7b, 58 ^b
3	5c	H	H/Me	Zn	6c, 22 ^b	7c, 57 ^b

^a*t*-Oct: (CH₃)₃CCH₂C(CH₃)₂. ^bSynthesized as a racemic mixture.

obtain reliable ECD spectra. As soon as the flow was turned off, the UV spectra of **6b** and **7b** changed significantly within seconds. It soon turned out that the free-base porphyrins were protonated by hydrochloric acid, which was formed by a porphyrin-catalyzed photodecomposition of the dichloromethane.⁴⁵ The measured ECD spectra of the protonated β -*meso* dimers were nearly identical to the ones described in the literature for another free-base β -*meso* dimer.¹³ Unfortunately, this meant that the determination of the absolute configuration had not been performed correctly and had to be repeated. Finally, ECD spectra of the unprotonated dimers and trimers were obtained by simply adding a base to the HPLC solvent (0.1% of HNEt₂ added to the *n*-hexane), which captured any acid formed by photodecomposition of the chlorinated solvent (Figures 6 and 7).

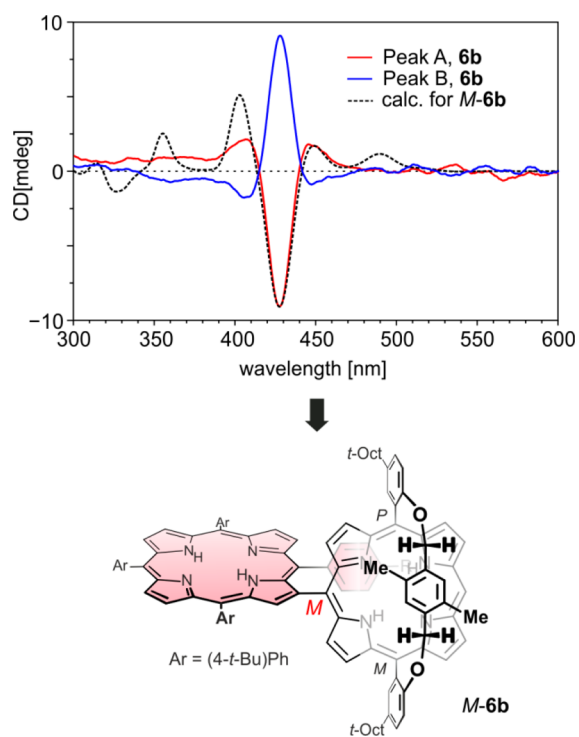


Figure 6. Determination of the absolute configurations of the β -*meso* linked dimer **6b** by comparison of the measured ECD spectra with the one calculated for the *M*-configured enantiomer of **6b** (sTD BHLYP/def2-SVP).

For an assignment of the absolute configurations of the dimers **6**, their ECD spectra measured online were compared with the sTD DFT calculated ones. Again, the simplified TD DFT approach gave ECD curves with good matches ($\Delta_{\text{ESI}} = 80\%$ for sTD CAM-B3LYP, $\Delta_{\text{ESI}} = 86\%$ for sTD BHLYP), and it was thus possible to attribute the *M* configuration to the enantiomers with a negative signal at 425 nm (Peak A), whereas the ones with a positive signal in this wavelength range were *P* configured (Figure 6).

The β -*meso* linked trimers **7b/c** are *C*₂-symmetric and planar-chiral. Because of this symmetry, the axes are not chiral for the trimers with a metalated BHP (**7c**) because descriptors of the porphyrin-porphyrin axes can only be assigned in case of a central free-base BHP with arrested tautomerism.²⁵ Still, it is important to describe the orientations of the *meso*-phenyl substituents directly adjacent to the axis: They are *cis* to each

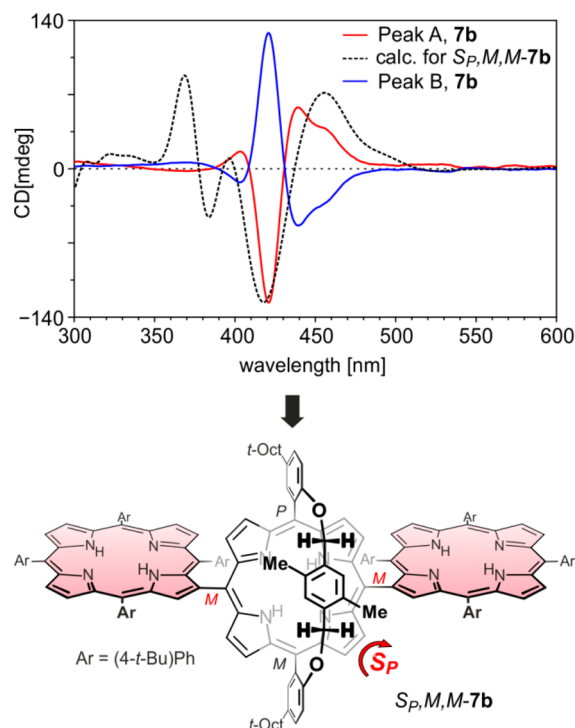


Figure 7. Elucidation of the absolute configurations of the enantiomers of the β -*meso* linked trimer **7b** by comparison of the calculated ECD spectra of *S_pM,M-7b* (sTD CAM-B3LYP/def2-SVP) with the experimental curves. Attribution of the axial stereodescriptors is possible only due to the arrested tautomerism in planar-chiral BHPs.

other but *trans* to the BHP strap. However, in the case of **7b** with the free-base BHP, the axes become chiral due to the arrested tautomerism of the BHP unit, which was previously described for planar-chiral free-base BHPs.²⁵

For an elucidation of the absolute configurations, sTD CAM-B3LYP/def2-SVP-calculated ECD spectra of the enantiomers of **7b** were compared with the ones experimentally obtained (Figure 7). The ECD curve calculated for *S_pM,M-7b*⁴⁶ showed a very good fit with that of the faster-eluting enantiomer, which was thus *S_pM,M* configured, and vice versa, the slower-eluting enantiomer had the *R_pP,P* configuration. The comparison of the ECD spectra of metalated and free-base trimers **7** showed, as expected, nearly no difference, and thus the absolute configurations (only concerning the planar chirality) succeeded by simple comparison of the experimental ECD curves (see Supporting Information).

Investigations of the Configurational Stability of β - β Linked Porphyrin Dimers. Previously described β - β linked dimers of tetraarylporphyrins had shown a strong dependence of the conformational stability of the axis on the metalation pattern of the porphyrin core.¹⁴ Although examples of Zn(II), Pd(II), and Cu(II) species were stereochemically stable even at elevated temperature, the Ni(II) and the free-base derivatives underwent rapid atrop-isomerization at room temperature. The β - β linked dimer **8**,²⁵ containing a BHP subunit, was found to adopt only the conformation with the *meso*-aryl moiety next to the axis *trans* to the handle of the BHP (Figure 8, top). Therefore, this was the first example of a free-base β - β linked dimer with axial chirality stable at room temperature, but the absolute stereostructure was not assigned initially. Meanwhile, the enantiomers of **8** were resolved by HPLC on a chiral phase, which permitted the measurement of ECD spectra. The

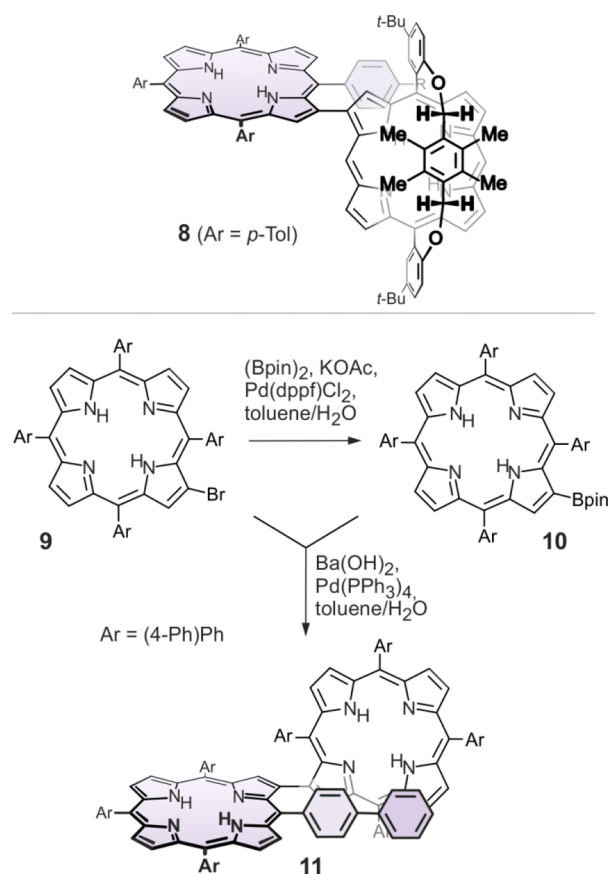


Figure 8. β - β linked bisporphyrin **8** with a BHP subunit (top); synthesis of the racemic β - β linked bisporphyrin **11** (bottom).

absolute configurations were assigned by comparison of the ECD curves with the ones of known β - β coupled dimers.¹⁴ In addition, sTD CAM-B3LYP calculations confirmed the

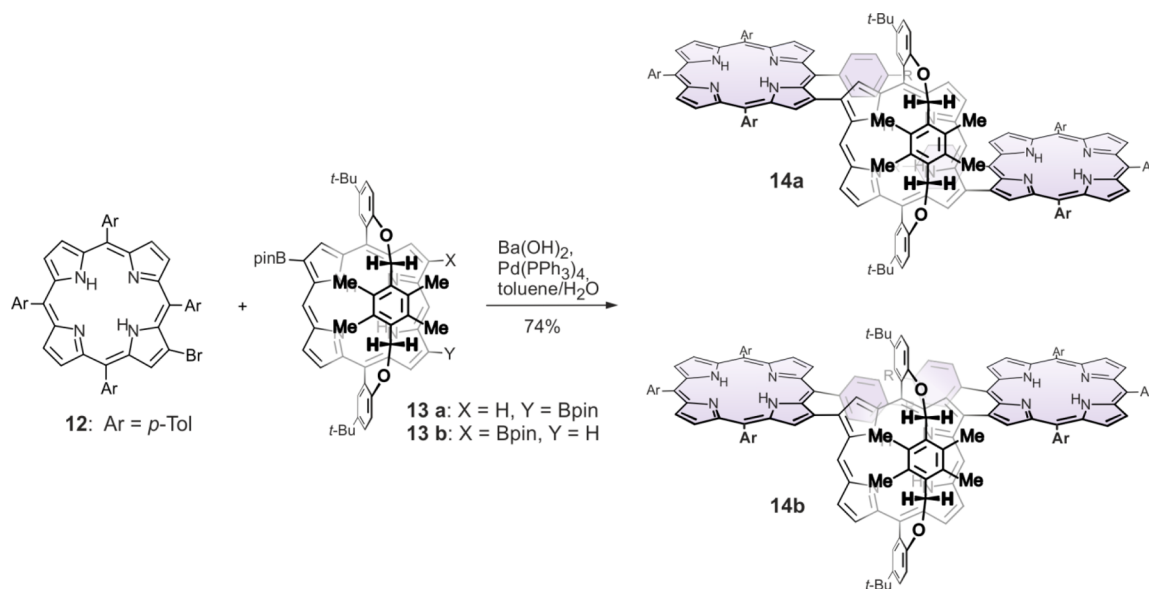
attributed absolute configurations (see Supporting Information).

Likewise synthesized was a configurationally stable free-base β - β coupled tetraarylbisporphyrin **11**. This dimer had *p*-biphenyl groups at the *meso* positions (Figure 8, bottom), so that, due to the drastically increased size of the *meso*-aryl unit compared to previous examples,¹⁴ the rotation at the β - β axis was fully hindered at room temperature. The enantiomers were resolvable by HPLC on a chiral phase, allowing us to measure ECD spectra in the stopped flow mode and subsequently to determine the absolute configurations of the enantiomers of **11** (see Supporting Information). The intensity of the ECD signal of **11** remained unchanged during repeated measurements over the course of 1 h, clearly indicating that there was no fast atropo-enantiomerization at room temperature.

Synthesis of β - β Linked Porphyrin Trimers by Suzuki Coupling of Functionalized BHPs. Although β -*meso* linked porphyrin trimers had been investigated thoroughly,^{13,27} no directed approach to β - β linked trimers had been reported. Yet, it should be possible to synthesize such trimers from known building blocks using the conditions previously reported for the synthesis of the first β - β linked dimer with a BHP subunit. Indeed, the Suzuki coupling of the β -brominated tetraporphyrin **12** with the β -borylated BHPs **13a/b** yielded two regioisomeric trimers **14a/b** (Scheme 2), but these trimers could not be resolved by column chromatography under various conditions.

For the Suzuki coupling, BHP **13** had been used as a 1:1 mixture of **13a** and **13b** (estimated by ¹H NMR, unseparable).³⁴ The product mixture was thus also found to consist of two compounds in a 1:1 ratio, each displaying a half set of signals in ¹H NMR. Symmetry considerations suggested a C_{2v}-symmetric structure for **14b** and a C₂-symmetric structure for **14a**. This was in agreement with the NMR data and with results from HPLC-ECD investigations because HPLC on a chiral phase yielded three peaks in a 1:2:1 ratio (Figure 9). Although all three peaks showed an identical UV spectrum, only the

Scheme 2. Suzuki Coupling of β -Borylated BHPs **13a/b** and β -Brominated Tetraporphyrin **12**^a



^aReaction of **12** with a 1:1 mixture of **13a** and **13b**; isolated yield of a 1:1 mixture of **14a** and **14b**; **14a** synthesized as a racemic mixture from **13a** (itself a racemic mixture); arbitrarily, only one enantiomer is shown.

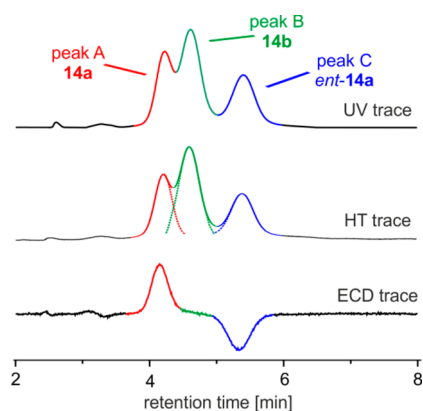


Figure 9. HPLC-ECD chromatograms (Chiralpak IA, *i*-propanol/*n*-hexane 15/85) of the product mixture **14a/b**; UV absorption, HT voltage, and ECD trace measured at 420 nm.

minor ones (peak A and peak C) displayed an ECD effect with opposite signs. The ECD spectra for all three peaks were measured in the stopped flow mode, and peaks A and C gave mirror imaged spectra, whereas for peak B no ECD effect was detectable. These findings strongly supported the proposed product structures.

Stereostructural Elucidation of β - β Linked Porphyrin Trimers. A conformational analysis using a C_2 -symmetry restriction yielded two different conformations for **14a**; additionally, one asymmetric (C_1) geometry had been considered (see Supporting Information). Although these conformations displayed significantly different angles at the porphyrin-porphyrin axes, their (calculated) ECD spectra were quite similar regarding the sign, but they had significantly different intensities (see Supporting Information). This was in contrast to the β -*meso* dimers and trimers, which showed conformations with nearly mirror-image-like ECD curves.

The sTD CAM-B3LYP/def2-SVP calculated overall spectra were compared with the experimentally measured ones and allowed the elucidation of the absolute configuration of **14a** (Figure 10). While the more rapidly eluting enantiomer (Peak A) with a negative Cotton effect at 415 nm was *P,P* configured at the porphyrin-porphyrin axes, the more slowly eluting one (Peak C) had the *M,M* configuration.

CONCLUSIONS

In this paper, we have demonstrated the potential of BHPs as building blocks for the construction of stereochemically intriguing structures with varying coupling types between the porphyrin units. Directly *meso-meso* linked BHP dimers with different outer *meso* substitution (*meso*-free, aryl, alkyl, halogen) and with different central metals [Ni(II), Pd(II), Cu(II), Zn(II)] were synthesized in mostly excellent yields by direct oxidative coupling. One of the Ni(II) dimers was further oxidized to a β - β , *meso-meso* fused system. Furthermore, dimers and trimers with direct β -*meso* and β - β linkages were synthesized by Suzuki coupling of suitably functionalized building blocks. Because of the steric hindrance of the BHP unit, these arrays were formed with full diastereoselectivity regarding all porphyrin-porphyrin axes, leading to the formation of products with an arrangement of the central aryl substituents *trans* to the handle. Thorough investigations regarding the chirality of all of these systems succeeded both experimentally and computationally, and a variety of examples with axial

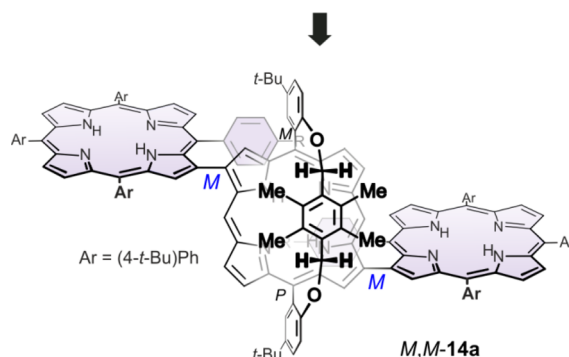
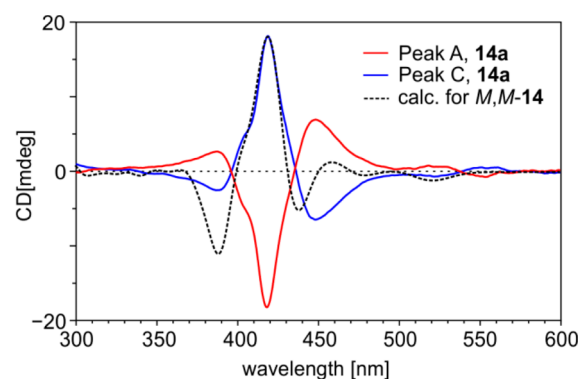


Figure 10. Determination of the absolute configurations of the β - β linked dimer **14a** by comparison of the measured ECD spectra with the one calculated for the *M,M*-configured enantiomer of **14a** (sTD B3LYP/def2-SVP).

chirality and/or planar chirality were presented along with one example with helical chirality. All racemic mixtures were resolved into their enantiomers by HPLC on a chiral phase, and their ECD spectra were recorded. By quantum-chemical ECD calculations, the absolute configurations of all reported dimeric and trimeric porphyrin arrays were assigned. For this task, the simplified TD DFT approach was extremely useful as it gave ECD spectra in good to excellent agreement with the experimental curves at comparably low computational costs. In summary, this work describes the synthetic access and the stereostructural properties of directly linked and fused dimeric and trimeric basket-handle porphyrins with examples of *meso-meso*, β -*meso*, and β - β coupling.

COMPUTATIONAL DETAILS

Initial optimizations were done with Turbomole⁴⁷ applying the B97-D3^{48–50} functional (including Becke-Johnson damping) and the def2-SVP⁵¹ basis set. Symmetry constraints were used where possible (C_2 symmetry for **M-2**, **7b**, and **14a**) and the *t*-butyl, *t*-octyl, or the tolyl-methyl groups have been replaced by hydrogens to save computational time. Single-point energy calculations (for the Boltzmann weighting of the spectra of **6b**, **7b**, **8**, and **14a**) were done in ORCA^{52,53} applying the chain-of-spheres⁵⁴ approximation and using the hybrid functional B3LYP-D3^{55,56} in combination with the def2-TZVP⁵¹ basis set and with a slightly increased Grid (Grid 5). All TD DFT calculations have been done with Gaussian09⁵⁷ using the functionals B3LYP, CAM-B3LYP,⁵⁸ and BHandHLYP (BHandHLYP keyword in G09) in combination with the def2-SVP⁵¹ basis set (def2-TZVP for bromine and metals atoms). The SCS-CC2⁵⁹ calculations of **Ni-3** were performed with Turbomole in combination with the def2-SVP basis set and using the RI

approximation. The molten files necessary for the sTD DFT^{41,60,61} calculations were generated from Gaussian09 log files with the g2molten script; the calculations themselves were done with the sTDA software provided by the Grimme group. Evaluation of the computed and experimental ECD spectra were done with SpecDis^{43,62} (results from length formalism) applying the following σ values and UV shifts:⁶³ Ni-2: $\sigma = 0.1$ eV for all methods; 50 nm (TD CAM-B3LYP); 30 nm (sTD CAM-B3LYP); 58 nm (TD BHLYP); 15 nm (sTD BHLYP); Δ_{ESI} was determined in the range from 300 to 600 nm. Ni-3: 0.2 eV, 45 nm (TD CAM-B3LYP); 0.2 eV, 33 nm (sTD CAM-B3LYP); 0.15 eV, 15 nm (TD B3LYP); 0.15 eV, 17 nm (sTD B3LYP); 0.19 eV, 8 nm (sTD BHLYP); 0.1 eV, 80 nm (SCS-CC2); Δ_{ESI} was determined in the range from 300 to 900 nm. 6b: 0.1 eV, 30 nm (sTD CAM-B3LYP); 0.07 eV, 13 nm (sTD BHLYP). 7b: 0.1 eV, 0 nm (sTD CAM-B3LYP); 0.1 eV, 25 nm (sTD BHLYP); Δ_{ESI} was determined in the range from 300 to 600 nm. 8: 0.1 eV, 17 nm (sTD CAM-B3LYP); 0.05 eV, 10 nm (sTD BHLYP); Δ_{ESI} was determined in the range from 300 to 600 nm. 14a: 0.11 eV, 32 nm (sTD CAM-B3LYP), 0.08 eV, 24 nm (sTD BHLYP); Δ_{ESI} was determined in the range from 300 to 600 nm. The monomeric BHPs were optimized using B97-D3/def2-TZVP and subsequent ω B97X-D3/def2-TZVP^{64,65} calculations yielded wave functions (all performed with ORCA using RI or RJCOSX), which were analyzed with multiwfn⁶⁶ to get the ALIE surfaces. For their visualization, a combination of VMD⁶⁷ and PovRay was used.

EXPERIMENTAL SECTION

General Considerations. All reagents were obtained from commercial sources and used as received, and all solvents were used as technical grade. Unless stated otherwise, all reactions were carried out in an atmosphere of dry nitrogen or argon using oven-dried (120 °C) glassware. Analytical TLCs were performed on ready-made plates coated with silica gel on aluminum and flash chromatography using silica gel 60 (230–400 mesh). ¹H and ¹³C NMR spectra were recorded in CDCl₃ at ambient temperature on spectrometers operating at 400 MHz for ¹H. ¹³C nucleus was observed with ¹H decoupling and solvent residual signals as internal standard. Chemical shifts (δ) and coupling constants (*J*) are given in ppm and Hz, respectively. The peak patterns are indicated as the following format multiplicity (s, singlet; d, doublet; t, triplet; q, quartet; m, multiplet; dd, doublet of doublets; dt, doublet of triplets; etc.). HRMS (ESI-TOF) spectra were measured in positive mode. Analytical enantiomeric resolution was performed on a standard HPLC system equipped with Diacel Chiralpak IA (4.6 × 250 mm; 3 μ m) as a chiral phase. Online ECD spectra were recorded at room temperature (scanning rate: 500 nm/min, bandwidth 5 or 10 nm, response time: 0.5s) by HPLC-ECD coupling in stopped-flow mode. Recycling gel permeation chromatography (recycling GPC) was performed on an HPLC System with two columns in line (SDV material, particle size 10 μ m, pore size 50 Å, dimension 20 × 600 mm and SDV material, particle size 10 μ m, pore size 100 Å, dimension 20 × 600 mm) at a flow rate of 4.5 mL/min in amylene-stabilized chloroform. Chromatographic details for the enantiomeric resolution of the chiral compounds are included in the Supporting Information. The *meso-meso* dimers in the Experimental Section are denoted by their compound number, and brief information regarding their substitution is added (R¹ = *meso*-substituent opposite the coupling site; R² = presence of solubilizing groups at the handle-bearing aryl group; R³/R⁴ = substituents of the xylene unit of the BHP, R³ = R⁴ for achiral BHPs and R³ ≠ R⁴ for chiral BHPs; M = coordinated metal ion)

General Procedure A: Oxidative Dimerization of Metallo-BHPs M-1²⁵ with PIFA. Metallo-BHP M-1²⁵ (100 μ mol, 1.0 equiv) was dissolved in dichloroethane (100 mL) and degassed with a stream of argon for 15 min. PIFA (26 mg, 60 μ mol, 0.6 equiv) was dissolved in abs. dichloroethane (5 mL) and added to the solution within 1 min.

As soon as the TLC reaction monitoring indicated full consumption of the starting material, the solution was filtered through a plug of silica and washed with chloroform, and all solvents were removed. The resulting solid was precipitated from chloroform/methanol to yield a purple powder. Ni-2a was further purified by recycling GPC. Zn-2f was not recrystallized but rather characterized immediately.

Dimer Ni-2a (R¹ = H, R² = *t*-Bu). Prepared from Ni-1a (82 mg); purified by recycling GPC. Purple powder, 18 mg, 22% yield; mp >350 °C. ¹H NMR (400 MHz, CDCl₃): δ 0.44 (s, 6H), 0.55 (s, 6H), 0.84 (s, 3H), 0.86 (s, 3H), 1.56 (s, 18H), 1.69 (s, 18H), 4.09 (d, ³J = 10.0 Hz, 2H), 4.18 (d, ³J = 10.1 Hz, 2H), 4.25 (d, ³J = 10.0 Hz, 2H), 4.31 (d, ³J = 10.1 Hz, 2H), 6.71 (d, ³J = 8.6 Hz, 2H), 6.82 (d, ³J = 8.6 Hz, 2H), 7.40 (d, ³J = 5.0 Hz, 2H), 7.52 (dd, ³J = 8.5, ⁴J = 2.5 Hz, 2H), 7.63 (dd, ³J = 8.5, ⁴J = 2.5 Hz, 2H), 8.30 (d, ³J = 5.0 Hz, 2H), 8.68 (d, ⁴J = 2.5 Hz, 2H), 8.74 (d, ³J = 4.8 Hz, 2H), 8.77 (d, ³J = 4.7 Hz, 2H), 8.80 (d, ³J = 4.9 Hz, 2H), 8.88 (dd, ³J = 4.8, ⁴J = 1.1 Hz, 4H), 8.94–8.97 (m, 4H), 9.48 (s, 2H). ¹³C NMR (100 MHz, CDCl₃): δ 14.8, 14.9, 15.1, 29.9, 32.0, 32.1, 32.1, 34.5, 34.7, 64.3, 64.4, 77.2, 103.8, 110.2, 110.3, 113.2, 113.4, 115.0, 126.2, 126.2, 127.4, 127.7, 128.3, 128.6, 131.40, 131.43, 131.7, 131.76, 131.83, 132.0, 132.2, 132.4, 132.7, 132.8, 134.2, 134.6, 140.9, 141.0, 141.7, 141.9, 142.0, 142.16, 142.20, 142.3, 143.6, 145.5, 156.4, 156.5. MS (MALDI, positive): *m/z* = 1638.572 [M]⁺. HRMS (ESI, positive) calcd for C₁₀₄H₉₈N₈Ni₂O₄ [M]⁺: 1638.6413; found, 1638.6430.

Dimer Ni-2b (R¹ = *n*-Bu, R² = H). Prepared from Ni-1b (76 mg). Purple powder, 74 mg, 97% yield; mp >350 °C. ¹H NMR (400 MHz, CDCl₃): δ 0.31 (s, 6H), 0.46 (s, 6H), 0.87–0.94 (m, 6H), 1.01 (s, 6H), 1.03 (s, 6H), 1.32–1.40 (m, 4H), 2.02 (m, 4H), 4.11 (d, ³J = 10.0 Hz, 2H), 4.20 (d, ³J = 10.0 Hz, 2H), 4.35 (d, ³J = 9.9 Hz, 2H), 4.40 (d, ³J = 10.0 Hz, 2H), 4.57 (t, ³J = 7.7 Hz, 4H), 6.76 (dd, ³J = 8.2, ⁴J = 1.0 Hz, 2H), 6.87 (dd, ³J = 8.2, ⁴J = 1.1 Hz, 2H), 7.28–7.33 (m, 4H), 7.42–7.49 (m, 4H), 7.57 (dd, ³J = 7.8, ⁴J = 1.8 Hz, 2H), 8.19 (d, ³J = 5.0 Hz, 2H), 8.55 (dd, ³J = 7.4, ⁴J = 1.7 Hz, 2H), 8.66 (d, ³J = 4.8 Hz, 2H), 8.70 (d, ³J = 4.9 Hz, 2H), 8.79–8.83 (m, 6H), 9.12 (d, ³J = 4.9 Hz, 2H), 9.18 (d, ³J = 5.0 Hz, 2H). ¹³C NMR (100 MHz, CDCl₃): δ 1.2, 14.1, 14.6, 14.9, 15.1, 15.2, 23.1, 29.9, 31.7, 32.0, 32.1, 32.2, 33.2, 38.4, 53.5, 64.2, 64.3, 77.2, 94.4, 110.8, 110.9, 112.9, 113.0, 113.8, 119.0, 119.2, 119.3, 127.5, 128.7, 129.0, 129.8, 130.0, 130.2, 130.3, 130.4, 130.4, 131.6, 131.6, 131.6, 131.7, 131.8, 131.9, 132.0, 132.0, 132.9, 133.0, 134.1, 134.7, 137.4, 140.4, 140.4, 140.8, 141.0, 141.4, 141.5, 144.1, 145.7, 158.6, 158.7. MS (MALDI, positive): *m/z* = 1526.497 [M]⁺. HRMS (ESI, positive) calcd for C₉₆H₈₂N₈Ni₂O₄ [M]⁺: 1526.5161; found, 1526.5149.

Dimer Ni-2c (R¹ = (4-*t*-Bu)Ph, R² = H). Prepared from Ni-1c (84 mg). Purple powder, 82 mg, 98% yield; mp >350 °C. ¹H NMR (400 MHz, CDCl₃): δ 0.52 (s, 6H), 0.66 (s, 6H), 0.95 (s, 6H), 0.97 (s, 6H), 1.54 (s, 18H), 4.16 (d, ³J = 10.0 Hz, 2H), 4.26 (d, ³J = 10.1 Hz, 2H), 4.31 (d, ³J = 10.0 Hz, 2H), 4.36 (d, ³J = 10.1 Hz, 2H), 6.77 (d, ³J = 8.3 Hz, 2H), 6.88 (d, ³J = 8.1 Hz, 2H), 7.30–7.34 (m, 2H), 7.42–7.50 (m, 4H), 7.58 (td, ³J = 7.9, ⁴J = 1.8 Hz, 2H), 7.65–7.70 (m, 4H), 7.92 (d, ³J = 7.6 Hz, 4H), 8.25 (d, ³J = 5.0 Hz, 2H), 8.55 (dd, ³J = 7.4, ⁴J = 1.7 Hz, 2H), 8.65 (s, 4H), 8.73 (dd, ³J = 4.9, ⁴J = 4.0 Hz, 4H), 8.77 (d, ³J = 4.9 Hz, 2H), 8.81 (d, ⁴J = 1.7 Hz, 1H), 8.83 (d, ³J = 4.9 Hz, 3H). ¹³C NMR spectrum could not be measured due to precipitation of Ni-2c from solvent after a few minutes. MS (MALDI, positive): *m/z* = 1678.512 [M]⁺. HRMS (ESI, positive) calcd for C₁₀₈H₉₀N₈Ni₂O₄ [M]⁺: 1678.5787; found, 1678.5781.

Dimer Ni-2d (R¹ = Br, R² = *t*-Bu). Prepared from Ni-1d (90 mg). Purple powder, 88 mg, 96% yield; mp >350 °C. ¹H NMR (400 MHz, CDCl₃): δ 0.35 (s, 6H), 0.45 (s, 6H), 1.15 (s, 6H), 1.17 (s, 6H), 1.54 (s, 18H), 1.67 (s, 18H), 4.10 (d, ³J = 10.0 Hz, 2H), 4.18 (d, ³J = 10.0 Hz, 2H), 4.37 (d, ³J = 9.9 Hz, 2H), 4.42 (d, ³J = 9.9 Hz, 2H), 6.73 (d, ³J = 8.6 Hz, 2H), 6.82 (d, ³J = 8.6 Hz, 2H), 7.05 (app t, ³J = 7.7 Hz, 1H), 7.35 (d, ³J = 5.0 Hz, 2H), 7.52 (dd, ³J = 8.5 Hz, ⁴J = 2.5 Hz, 2H), 7.62 (dd, ³J = 8.5 Hz, ⁴J = 2.5 Hz, 2H), 7.68 (dd, ³J = 8.4 Hz, ⁴J = 1.2 Hz, 1H), 8.22 (d, ³J = 4.9 Hz, 2H), 8.60 (d, ⁴J = 2.5 Hz, 2H), 8.66 (d, ³J = 4.9 Hz, 2H), 8.70 (d, ³J = 5.0 Hz, 2H), 8.78 (d, ³J = 4.9 Hz, 2H), 8.81 (d, ³J = 5.0 Hz, 2H), 8.87 (d, ⁴J = 2.5 Hz, 2H), 9.24 (d, ³J = 4.9 Hz, 2H), 9.31 (d, ³J = 5.0 Hz, 2H). ¹³C NMR (100 MHz, CDCl₃): δ

18H), 1.34 (s, 18H), 1.52 (s, 6H), 1.57 (s, 6H), 1.62 (s, 18H), 1.69 (s, 18H), 1.92 (d, $^3J = 14.2$ Hz, 2H), 2.03 (d, $^3J = 14.3$ Hz, 2H), 2.19 (d, $^3J = 14.4$ Hz, 2H), 3.45–3.56 (m, 4H), 5.46 (d, $^3J = 7.8$ Hz, 2H), 6.61 (d, $^3J = 7.9$ Hz, 2H), 6.72 (d, $^3J = 7.8$ Hz, 2H), 7.00 (d, $^3J = 8.5$ Hz, 2H), 7.35 (d, $^3J = 4.8$ Hz, 2H), 7.48 (d, $^3J = 7.9$ Hz, 2H), 7.51–7.55 (m, 2H), 7.58–7.64 (m, 1H), 7.78 (d, $^3J = 7.5$ Hz, 4H), 7.83–7.93 (m, 5H), 8.11–8.19 (m, 1H), 8.23–8.28 (m, 7H), 8.38 (t, $^3J = 4.8$ Hz, 4H), 8.49 (d, $^3J = 4.8$ Hz, 2H), 8.78 (d, $^3J = 4.8$ Hz, 2H), 8.82 (d, $^4J = 2.5$ Hz, 2H), 8.93 (d, $^3J = 4.8$ Hz, 2H), 8.96 (d, $^3J = 4.8$ Hz, 2H), 9.07 (d, $^3J = 4.8$ Hz, 2H), 9.15 (d, $^3J = 4.8$ Hz, 2H), 9.19 (d, $^3J = 4.7$ Hz, 2H), 9.39 (s, 2H). ^{13}C NMR (100 MHz, CDCl_3) δ 1.2, 14.3, 15.2, 19.9, 22.8, 22.9, 22.9, 24.6, 27.3, 29.5, 29.8, 29.9, 29.9, 30.2, 30.4, 31.5, 31.6, 31.8, 31.9, 32.1, 32.1, 32.2, 32.8, 32.9, 33.3, 34.8, 35.0, 35.1, 37.3, 37.6, 38.5, 57.4, 72.8, 113.2, 115.5, 120.2, 120.3, 120.4, 120.8, 121.4, 121.9, 122.5, 123.8, 123.9, 126.0, 127.1, 127.6, 129.4, 130.1, 130.3, 130.5, 131.3, 133.8, 134.8, 134.8, 134.9, 136.8, 137.3, 139.3, 139.4, 139.4, 141.0, 144.5, 148.4, 149.9, 150.6, 150.6, 150.7, 153.0, 158.8. MS (MALDI, positive): $m/z = 2521.454$ [M] $^{+}$. HRMS (ESI, positive) calcd for $\text{C}_{178}\text{H}_{184}\text{N}_{12}\text{O}_2$ [M] $^{+}$: 2521.4660; found, 2521.4668.

Dimer 6c and Trimer 7c ($\text{R}^2 = \text{H}$, $\text{R}^3 = \text{H}$, $\text{R}^4 = \text{Me}$, Tetra-(*t*-Bu)Ph-porphyrin, $\text{M} = 2\text{H}-\text{Zn}-2\text{H}$). Synthesized from **4a** (96 mg) and **5c** (54 mg).

6c: 19 mg, 22%; mp >350 °C. ^1H NMR (400 MHz, CDCl_3) δ -2.33 (s, 2H), -1.13 (s, 9H), -0.87 (s, 3H), -0.33 (s, 3H), 1.37 (s, 9H), 1.66 (s, 9H), 2.09 (d, $^3J = 14.1$ Hz, 1H), 2.19 (d, $^3J = 14.1$ Hz, 1H), 3.26 (s, 1H), 3.35 (d, $^3J = 14.0$ Hz, 1H), 3.42 (d, $^3J = 14.4$ Hz, 1H), 3.56 (s, 1H), 4.90–5.00 (m, 2H), 6.67 (dd, $^3J = 7.5$ Hz, $^4J = 2.2$ Hz, 2H), 6.73 (dd, $^3J = 7.7$ Hz, $^4J = 2$ Hz, 1H), 7.07 (ddd, $^3J = 11.4$ Hz, $^3J = 8.0$ Hz, $^4J = 1.2$ Hz, 2H), 7.56–7.65 (m, 2H), 7.71 (td, $^3J = 6.9$ Hz, $^3J = 6.5$ Hz, $^4J = 1.6$ Hz, 5H), 7.84 (d, $^3J = 7.8$ Hz, 2H), 7.95–8.02 (m, 1H), 8.07–8.17 (m, 3H), 8.26 (d, $^3J = 7.8$ Hz, 3H), 8.41 (d, $^3J = 7.9$ Hz, 2H), 8.49 (d, $^3J = 4.5$ Hz, 1H), 8.60–8.65 (m, 3H), 8.69 (d, $^3J = 4.5$ Hz, 1H), 8.85 (dd, $^3J = 4.5$ Hz, $^4J = 1.8$ Hz, 2H), 8.89 (d, $^3J = 4.9$ Hz, 1H), 8.93 (d, $^3J = 4.8$ Hz, 1H), 8.98–9.08 (m, 3H), 9.11 (d, $^3J = 4.8$ Hz, 1H), 9.20 (d, $^3J = 4.5$ Hz, 1H), 9.28 (d, $^3J = 4.5$ Hz, 1H), 9.33 (d, $^3J = 4.4$ Hz, 1H), 9.64 (s, 1H), 10.03 (s, 1H). ^{13}C NMR (100 MHz, CDCl_3): δ 13.0, 13.5, 14.3, 22.8, 27.2, 29.1, 29.5, 29.8, 31.7, 31.8, 31.9, 32.1, 32.1, 34.8, 35.0, 35.1, 39.3, 63.7, 104.5, 106.6, 110.9, 115.4, 119.5, 120.3, 120.4, 120.7, 122.4, 123.6, 123.6, 123.8, 127.1, 128.6, 128.7, 129.6, 130.5, 130.9, 130.9, 131.4, 131.5, 132.0, 132.1, 132.2, 132.2, 132.3, 132.9, 132.9, 133.2, 134.6, 134.8, 134.9, 136.8, 139.3, 139.4, 139.8, 146.7, 147.4, 149.0, 150.2, 150.4, 150.6, 150.7, 151.1, 155.0, 158.7. MS (MALDI, positive): $m/z = 1522.664$ [M] $^{+}$. HRMS (ESI, positive) calcd for $\text{C}_{102}\text{H}_{90}\text{N}_8\text{O}_2\text{Zn}$ [M] $^{+}$: 1522.6473; found, 1522.6481.

7c: 73 mg, 57%; mp >350 °C. ^1H NMR (400 MHz, CDCl_3): δ -2.20 (s, 4H), -0.49 (s, 6H), 0.12 (s, 18H), 1.31 (s, 18H), 1.60 (s, 18H), 1.67 (s, 18H), 2.01 (d, $^3J = 14.2$ Hz, 2H), 3.40 (d, $^3J = 14.3$ Hz, 2H), 3.50 (s, 2H), 5.43 (s, 2H), 6.44 (s, 2H), 7.06 (dd, $^3J = 8.0$ Hz, $^4J = 1.3$ Hz, 2H), 7.41–7.46 (m, 2H), 7.52 (td, $^3J = 7.8$ Hz, $^4J = 1.8$ Hz, 2H), 7.57–7.66 (m, 4H), 7.76 (d, $^3J = 7.9$ Hz, 4H), 7.85 (d, $^3J = 7.6$ Hz, 5H), 8.13 (br s, 2H), 8.25 (br s, 6H), 8.31 (br s, 2H), 8.37 (d, $^3J = 4.8$ Hz, 2H), 8.44 (d, $^3J = 4.6$ Hz, 2H), 8.55 (d, $^3J = 4.8$ Hz, 2H), 8.73 (d, $^3J = 4.8$ Hz, 2H), 8.76 (d, $^4J = 1.8$ Hz, 1H), 8.77 (d, $^4J = 1.8$ Hz, 1H), 8.91 (d, $^3J = 4.8$ Hz, 2H), 8.94 (d, $^3J = 4.8$ Hz, 2H), 9.04 (d, $^3J = 4.8$ Hz, 2H), 9.11 (d, $^3J = 4.8$ Hz, 2H), 9.22 (d, $^3J = 4.6$ Hz, 2H), 9.43 (s, 2H). ^{13}C NMR (100 MHz, CDCl_3): δ 15.2, 29.9, 30.3, 31.4, 31.6, 31.8, 31.9, 33.2, 34.8, 35.0, 35.1, 39.2, 72.1, 106.6, 113.9, 120.3, 120.4, 120.6, 121.3, 121.8, 122.0, 123.4, 123.7, 123.9, 126.4, 129.6, 129.7, 130.5, 132.9, 134.2, 134.7, 134.9, 136.3, 137.3, 139.3, 139.4, 139.5, 148.4, 148.8, 149.5, 150.5, 150.7, 150.7, 150.7, 150.9, 154.4, 160.9. MS (MALDI, positive): $m/z = 2359.070$ [M] $^{+}$. HRMS (ESI, positive) calcd for $\text{C}_{162}\text{H}_{150}\text{N}_{12}\text{O}_2\text{Zn}$ [M] $^{+}$: 2359.1291; found, 2359.1296.

2-(4,4,5,5-Tetramethyl-[1,3,2]dioxaborolan-2-yl)-5,10,15,20-tetra(4-biphenyl)porphyrin (10). **5,10,15,20-Tetra(4-biphenyl)porphyrin**⁶⁸ (1.00 g, 1.09 mmol) was dissolved in 1,2-dichlorobenzene (200 mL) and heated to 160 °C. NBS (200 mg, 1.12 mmol) was added, and the solution was stirred at 160 °C for 45 min. MeOH (300 mL) was added at room temperature, and the precipitate was filtered off. TLC indicated a 1/2 ratio of remaining starting material to β -

brominated porphyrin **9**. Purification and characterization was not possible due to the extremely limited solubility of the mixture. Therefore, the mixture was directly subjected to the borylation. The porphyrin mixture (900 mg), (Bpin)₂ (260 mg, 0.95 mmol), and KOAc (370 mg, 3.79 mmol) were dissolved in toluene (100 mL) and water (20 mL) and degassed with an argon stream in an ultrasonic bath for 15 min. Pd(dppf)Cl₂ (31 mg, 0.038 mmol) was added, and the mixture was degassed for a further 20 min. Then, the reaction was heated to 110 °C for 24 h. After cooling to rt, the organic phase was filtered over a plug of silica (only borylated porphyrin **10** was soluble and thus eluted) and washed with ethyl acetate. After evaporation of all solvents, the residue was purified by column chromatography (silica, dichloromethane/methanol 1/0 → 9/1). The product was recrystallized from chloroform/methanol to yield a purple solid; 522 mg, 46% (over two steps); mp >300 °C. ^1H NMR (400 MHz, CDCl_3): δ -2.51 (s, 2H), 1.20 (s, 12H), 7.46–7.51 (m, 5H), 7.56–7.66 (m, 10H), 7.86–8.07 (m, 20H), 8.29–8.40 (m, 9H), 8.80 (d, $^3J = 4.9$ Hz, 1H), 8.88 (d, $^3J = 4.9$ Hz, 1H), 8.94 (d, $^3J = 4.2$ Hz, 4H), 9.25 (s, 1H). ^{13}C NMR (150 MHz, CDCl_3): δ 25.4, 84.0, 119.7, 119.9, 120.1, 121.7, 125.5, 125.5, 125.6, 125.6, 127.4, 127.5, 127.5, 127.7, 127.8, 129.2, 129.2, 135.3, 135.4, 135.6, 137.0, 140.4, 140.5, 140.6, 141.0, 141.0, 141.2, 141.5, 141.5, 142.5. MS (MALDI, positive): $m/z = 1044.381$ [M] $^{+}$. HRMS (ESI, positive) calcd for $\text{C}_{74}\text{H}_{58}\text{BN}_4\text{O}_2$ [$\text{M} + \text{H}$] $^{+}$: 1045.4647; found, 1045.4644.

β -Brominated Porphyrin 11. Porphyrin **9** (250 mg, ~2:1 mixture of β -brominated porphyrin **9** and 5,10,15,20-tetra(4-biphenyl)porphyrin), porphyrin **10** (100 mg, 95 μmol , 1 equiv), and Ba(OH)₂ (730 mg, 2.0 mmol) were dissolved in toluene (150 mL) and water (30 mL) and degassed with an argon stream in an ultrasonic bath for 15 min. Pd(PPh₃)₄ (15 mg, 15 μmol) was added, and the mixture was degassed for a further 20 min. Then, the reaction was heated to 110 °C for 15 h. After cooling to rt, the organic phase was filtered over a plug of silica and eluted with ethyl acetate. After evaporation of all solvents, the residue was purified by column chromatography (silica, *n*-hexane/dichloromethane 2/1 → 0/1). The product was recrystallized from chloroform/methanol to yield a purple-brown solid; 125 mg, 71%; mp >300 °C. ^1H NMR (400 MHz, CDCl_3): δ -2.58 (s, 4H), 4.00 (d, $^3J = 7.7$ Hz, 2H), 4.74 (d, $^3J = 7.7$ Hz, 4H), 6.21 (t, $^3J = 7.7$ Hz, 4H), 6.52 (d, $^3J = 7.7$ Hz, 2H), 6.63 (d, $^3J = 7.8$ Hz, 2H), 6.78 (t, $^3J = 7.4$ Hz, 2H), 7.32 (dd, $^3J = 7.8$ Hz, $^4J = 1.9$ Hz, 2H), 7.39–7.47 (m, 5H), 7.49–7.59 (m, 12H), 7.62–7.69 (m, 5H), 7.83–7.96 (m, 16H), 7.96–8.08 (m, 12H), 8.18 (d, $^3J = 4.8$ Hz, 4H), 8.23 (d, $^3J = 7.2$ Hz, 2H), 8.26–8.33 (m, 2H), 8.37 (dd, $^3J = 7.6$ Hz, $^4J = 1.6$ Hz, 2H), 8.40 (d, $^3J = 7.7$ Hz, 2H), 8.56 (d, $^3J = 7.7$ Hz, 2H), 8.68 (d, $^3J = 4.8$ Hz, 2H), 8.76 (d, $^3J = 4.8$ Hz, 2H), 8.94 (d, $^3J = 4.8$ Hz, 2H), 8.95–9.03 (m, 6H). ^{13}C NMR measurements were not successful due to the limited solubility of the product. MS (MALDI, positive): $m/z = 1834.812$ [M] $^{+}$. HRMS (ESI, positive) calcd for $\text{C}_{136}\text{H}_{91}\text{N}_8$ [$\text{M} + \text{H}$] $^{+}$: 1835.7361; found, 1835.7359.

Suzuki Coupling of β -brominated Tetraarylporphyrin 12 with β -Borylated BHPs 13a/b. Porphyrin **12** (150 mg, 200 μmol , 2 equiv), porphyrins **13a/b** (102 mg, 100 μmol , 1 equiv), and Ba(OH)₂ (730 mg, 2.0 mmol) were dissolved in toluene (150 mL) and water (30 mL) and degassed with an argon stream in an ultrasonic bath for 15 min. Pd(PPh₃)₄ (15 mg, 15 μmol) was added, and the mixture was degassed for a further 20 min. Then, the reaction was heated to 110 °C for 15 h. After cooling to rt, the organic phase was filtered over a plug of silica and fully eluted with ethyl acetate. After evaporation of all solvents, the residue was purified by column chromatography (silica, *n*-hexane/dichloromethane 2/1 → 0/1), which yielded a mixture of the trimers **14a/b** (1:1 ratio estimated by ^1H NMR). Further attempts to resolve the stereoisomers by column chromatography failed. Mixture of trimers **14a/b** ($\text{R}^2 = t\text{-Bu}$, $\text{R}^3 = \text{R}^4 = \text{Me}$, tetra-(4-Me)Ph-porphyrin, $\text{M} = 2\text{H}-2\text{H}-2\text{H}$), 125 mg, 71%; mp >300 °C. ^1H NMR (400 MHz, CDCl_3): δ -2.82 (s, 2H), -2.51 (s, 2H), -2.33 (s, 4H), -2.28 (s, 4H), -0.04 (s, 6H), -0.01 (s, 6H), 0.11 (s, 6H), 0.18 (s, 6H), 1.27 (s, 6H), 1.43 (s, 6H), 1.73 (s, 9H), 1.77 (s, 18H), 1.78 (s, 9H), 2.48 (s, 6H), 2.52 (s, 6H), 2.72 (s, 6H), 2.74 (s, 6H), 2.75 (s, 6H), 2.79 (s, 6H), 3.52 (s, 2H), 3.67 (d, $^3J = 11.3$ Hz, 4H), 3.72 (d, $^3J = 10.3$ Hz, 2H), 5.00 (d, $^3J = 7.7$ Hz, 2H), 6.44 (d, $^3J = 8.5$ Hz, 1H), 6.56 (d, $^3J =$

8.6 Hz, 2H), 6.61 (d, $^3J = 8.5$ Hz, 1H), 7.50–7.71 (m, 26H), 8.08–8.33 (m, 32H), 8.46 (s, 2H), 8.57 (s, 1H), 8.70 (s, 4H), 8.78 (s, 5H), 8.80 (d, $^3J = 7.2$ Hz, 2H), 8.83 (d, $^3J = 4.8$ Hz, 2H), 8.87 (d, $^3J = 4.9$ Hz, 2H), 8.94 (d, $^3J = 4.8$ Hz, 3H), 8.96 (d, $^3J = 4.9$ Hz, 5H), 8.99 (s, 2H), 9.01 (d, $^3J = 4.9$ Hz, 3H), 9.05 (d, $^3J = 4.7$ Hz, 2H), 9.09 (d, $^4J = 2.5$ Hz, 2H), 9.12 (s, 2H), 9.27 (s, 2H), 9.61 (s, 2H), 9.68 (s, 2H). ^{13}C NMR spectra were not interpretable due to the product being present as a mixture of two isomers. MS (MALDI, positive): $m/z = 2101.023$ $[\text{M}]^+$. HRMS (ESI, positive) calcd for $\text{C}_{148}\text{H}_{125}\text{N}_{12}\text{O}_2$ $[\text{M} + \text{H}]^+$: 2102.0043; found, 2102.0050.

■ ASSOCIATED CONTENT

Supporting Information

The Supporting Information is available free of charge on the ACS Publications website at DOI: 10.1021/acs.joc.5b02638.

^1H and ^{13}C NMR, VT NMR of **7a**, chromatographic details for the enantiomeric resolution of **Ni-2a**, **Ni-2b**, **Ni-2c**, **Ni-2d**, **Pd-2e**, **Cu-2c**, **Ni-3**, **6b**, **6c**, **7b**, **7c**, **8**, **11**, and **14a**, UV/vis spectra, comparisons of experimental and calculated ECD spectra, ALIE surfaces, and Cartesian Coordinates and energies of the computationally investigated compounds (PDF)
Crystallographic Data for **Cu-1c** (CIF)

■ AUTHOR INFORMATION

Corresponding Authors

*E-mail: torsten.bruhn@uni-wuerzburg.de.

*E-mail: bringman@chemie.uni-wuerzburg.de.

Notes

The authors declare no competing financial interest.

■ ACKNOWLEDGMENTS

The authors gratefully acknowledge F. Witterauf for support with the ECD measurements, S. Schmitt for experimental support with the BHP synthesis, and H. Schneider and U. Radius for providing the X-ray structure of **Cu-1c**.

■ REFERENCES

- Tanaka, T.; Osuka, A. *Chem. Soc. Rev.* **2015**, *44*, 943.
- Aratani, N.; Kim, D.; Osuka, A. *Acc. Chem. Res.* **2009**, *42*, 1922.
- Fox, S.; Boyle, R. W. *Tetrahedron* **2006**, *62*, 10039.
- Aratani, N.; Kim, D.; Osuka, A. *Chem. - Asian J.* **2009**, *4*, 1172.
- Osuka, A.; Shimidzu, H. *Angew. Chem., Int. Ed. Engl.* **1997**, *36*, 135.
- Tsuda, A.; Nakano, A.; Furuta, H.; Yamochi, H.; Osuka, A. *Angew. Chem., Int. Ed.* **2000**, *39*, 558.
- Tsuda, A.; Furuta, H.; Osuka, A. *Angew. Chem., Int. Ed.* **2000**, *39*, 2549.
- Sahoo, A. K.; Nakamura, Y.; Aratani, N.; Kim, K. S.; Noh, S. B.; Shinokubo, H.; Kim, D.; Osuka, A. *Org. Lett.* **2006**, *8*, 4141.
- Feng, C.-M.; Zhu, Y.-Z.; Zang, Y.; Tong, Y.-Z.; Zheng, J.-Y. *Org. Biomol. Chem.* **2014**, *12*, 6990.
- Jin, L.-M.; Chen, L.; Yin, J.-J.; Guo, C.-C.; Chen, Q.-Y. *Eur. J. Org. Chem.* **2005**, *2005*, 3994.
- Ogawa, T.; Ogawa, T.; Nishimoto, Y.; Ono, N.; Yoshida, N.; Osuka, A. *Chem. Commun.* **1998**, 337.
- Lu, X.-Q.; Guo, Y.; Chen, Q.-Y. *Synlett* **2011**, *2011*, 77.
- Götz, D. C. G.; Bruhn, T.; Senge, M. O.; Bringmann, G. *J. Org. Chem.* **2009**, *74*, 8005.
- Bringmann, G.; Götz, D. C. G.; Gulder, T. A. M.; Gehrke, T. H.; Bruhn, T.; Kupfer, T.; Radacki, K.; Braunschweig, H.; Heckmann, A.; Lambert, C. *J. Am. Chem. Soc.* **2008**, *130*, 17812.
- Ryan, A.; Gehrold, A.; Perusitti, R.; Pintea, M.; Fazekas, M.; Locos, O. B.; Blaikie, F.; Senge, M. O. *Eur. J. Org. Chem.* **2011**, *2011*, 5817.
- Senge, M. O.; Feng, X. *Tetrahedron Lett.* **1999**, *40*, 4165.
- Hiroto, S.; Osuka, A. *J. Org. Chem.* **2005**, *70*, 4054.
- Yamamura, T.; Mori, T.; Tsuda, Y.; Taguchi, T.; Josha, N. *J. Phys. Chem. A* **2007**, *111*, 2128.
- Ahn, T. K.; Kim, K. S.; Kim, D. Y.; Noh, S. B.; Aratani, N.; Ikeda, C.; Osuka, A.; Kim, D. *J. Am. Chem. Soc.* **2006**, *128*, 1700.
- Hwang, I.-W.; Kamada, T.; Ahn, T. K.; Ko, D. M.; Nakamura, T.; Tsuda, A.; Osuka, A.; Kim, D. *J. Am. Chem. Soc.* **2004**, *126*, 16187.
- Hwang, I.-W.; Cho, H. S.; Jeong, D. H.; Kim, D.; Tsuda, A.; Nakamura, T.; Osuka, A. *J. Phys. Chem. B* **2003**, *107*, 9977.
- Tsuda, A.; Nakamura, T.; Sakamoto, S.; Yamaguchi, K.; Osuka, A. *Angew. Chem., Int. Ed.* **2002**, *41*, 2817.
- Shinmori, H.; Osuka, A. *Tetrahedron Lett.* **2000**, *41*, 8527.
- Yoshida, N.; Osuka, A. *Tetrahedron Lett.* **2000**, *41*, 9287.
- Gehrold, A. C.; Bruhn, T.; Schneider, H.; Radius, U.; Bringmann, G. *J. Org. Chem.* **2015**, *80*, 12359.
- Muranaka, A.; Asano, Y.; Tsuda, A.; Osuka, A.; Kobayashi, N. *ChemPhysChem* **2006**, *7*, 1235.
- Bruhn, T.; Witterauf, F.; Götz, D. C. G.; Grimmer, C. T.; Würtenberger, M.; Radius, U.; Bringmann, G. *Chem. - Eur. J.* **2014**, *20*, 3998.
- Tsuda, A.; Furuta, H.; Osuka, A. *J. Am. Chem. Soc.* **2001**, *123*, 10304.
- Kullmann, M.; Hipke, A.; Nuernberger, P.; Bruhn, T.; Götz, D. C. G.; Sekita, M.; Guldi, D. M.; Bringmann, G.; Brixner, T. *Phys. Chem. Chem. Phys.* **2012**, *14*, 8038.
- Takeuchi, M.; Fujikoshi, C.; Kubo, Y.; Kaneko, K.; Shinkai, S. *Angew. Chem., Int. Ed.* **2006**, *45*, 5494.
- Zhou, Z.; Shen, M.; Cao, C.; Liu, Q.; Yan, Z. *Chem. - Eur. J.* **2012**, *18*, 7675.
- Zhou, Z.; Cao, C.; Liu, Q.; Jiang, R. *Org. Lett.* **2010**, *12*, 1780.
- Urbani, M.; Torres, T. *Chem. - Eur. J.* **2014**, *20*, 16337.
- Gehrold, A. C.; Bruhn, T.; Schneider, H.; Radius, U.; Bringmann, G. *Org. Lett.* **2015**, *17*, 210.
- Ouyang, Q.; Zhu, Y.-Z.; Zhang, C.-H.; Yan, K.-Q.; Li, Y.-C.; Zheng, J.-Y. *Org. Lett.* **2009**, *11*, 5266.
- Ryan, A. A.; Senge, M. O. *Eur. J. Org. Chem.* **2013**, *2013*, 3700.
- Lebedeva, N. S.; Pavlycheva, N. A.; V'yugin, A. I. *Russ. J. Gen. Chem.* **2007**, *77*, 629.
- Zaitseva, S. V.; Zdanovich, S. A.; Koifman, O. I. *Russ. J. Gen. Chem.* **2005**, *75*, 800.
- Brown, J. J.; Cockroft, S. L. *Chem. Sci.* **2013**, *4*, 1772.
- Götz, D. C. G.; Gehrold, A. C.; Dorazio, S. J.; Daddario, P.; Samankumara, L.; Bringmann, G.; Brückner, C.; Bruhn, T. *Eur. J. Org. Chem.* **2015**, *2015*, 3913.
- Risthaus, T.; Hansen, A.; Grimme, S. *Phys. Chem. Chem. Phys.* **2014**, *16*, 14408.
- For an intriguing case of a chiral axis between two planar-chiral aryl entities, see: Tochtermann, W.; Kuckling, D.; Meints, C.; Kraus, J.; Bringmann, G. *Tetrahedron* **2003**, *59*, 7791.
- Bruhn, T.; Schaumlöffel, A.; Hemberger, Y.; Bringmann, G. *Chirality* **2013**, *25*, 243.
- Note that instead of the formally correct expression “*p*-xylylene”, the commonly found term “*p*-xylene” is used throughout the paper.
- Munoz, Z.; Cohen, A. S.; Nguyen, L. M.; McIntosh, T. A.; Hoggard, P. E. *Photochem. Photobiol. Sci.* **2008**, *7*, 337.
- In these cases, the usual *M/P* notation for the descriptors of the planar chirality is avoided for reasons of easier distinction of the planar-chiral from the axially chiral domains. For the chiral, free-base BHPs, the descriptors of the axis connecting the porphyrin to the handle-bearing aryl group are determined in a way that the pyrrole ring of the BHP containing the NH is given priority over the pyrrole ring without the NH.
- Ahrlrichs, R.; Armbruster, M. K.; Bachorz, R. A.; Bär, M.; Baron, H.-P.; Bauernschmitt, R.; Bischoff, F. A.; Böcker, S.; Crawford, N.; Deglmann, P.; Della Sala, F.; Diedenhofen, M.; Ehrig, M.; Eichkorn, K.; Elliott, S.; Friese, D.; Furche, F.; Glöß, A.; Haase, F.; Häser, M.; Hättig, C.; Hellweg, A.; Höfener, S.; Horn, H.; Huber, C.; Huniar, U.; Kattaneck, M.; Kloppe, W.; Köhn, A.; Kölmel, C.; Kollwitz, M.; May,

K.; Nava, P.; Ochsenfeld, C.; Öhm, H.; Pabst, M.; Patzelt, H.; Rappoport, D.; Rubner, O.; Schäfer, A.; Schneider, U.; Sierka, M.; Tew, D. P.; Treutler, O.; Unterreiner, B.; von Arnim, M.; Weigend, F.; Weis, P.; Weiss, H.; Winter, N.; *TURBOMOLE*, version 6.6; TURBOMOLE GmbH: Karlsruhe, Germany, 2014.

- (48) Grimme, S. *J. Comput. Chem.* **2006**, *27*, 1787.
- (49) Grimme, S.; Ehrlich, S.; Goerigk, L. *J. Comput. Chem.* **2011**, *32*, 1456.
- (50) Grimme, S.; Antony, J.; Ehrlich, S.; Krieg, H. *J. Chem. Phys.* **2010**, *132*, 154104.
- (51) Weigend, F.; Ahlrichs, R. *Phys. Chem. Chem. Phys.* **2005**, *7*, 3297.
- (52) Neese, F.; Wennmohs, F.; Becker, U.; Bykov, D.; Ganyushin, D.; Hansen, A.; Izšák, R.; Liakos, D. G.; Kollmar, C.; Kossmann, S.; Pantazis, D. A.; Petrenko, T.; Reimann, C.; Riplinger, C.; Roemelt, M.; Sandhöfer, B.; Schapiro, I.; Sivalingam, K.; Weizsäcker, B.; ORCA, version 3.0.3; MPI CEC: Mühlheim a.d.R., Germany, 2014.
- (53) Neese, F. *WIREs Comput. Mol. Sci.* **2012**, *2*, 73.
- (54) Izsak, R.; Neese, F. *J. Chem. Phys.* **2011**, *135*, 144105.
- (55) Becke, A. D. *J. Chem. Phys.* **1993**, *98*, 1372.
- (56) Lee, C.; Yang, W.; Parr, R. G. *Phys. Rev. B: Condens. Matter Mater. Phys.* **1988**, *37*, 785.
- (57) Frisch, M. J.; Trucks, G. W.; Schlegel, H. B.; Scuseria, G. E.; Robb, M. A.; Cheeseman, J. R.; Scalmani, G.; Barone, V.; Mennucci, B.; Petersson, G. A.; Nakatsuji, H.; Caricato, M.; Li, X.; Hratchian, H. P.; Izmaylov, A. F.; Bloino, J.; Zheng, G.; Sonnenberg, J. L.; Hada, M.; Ehara, M.; Toyota, K.; Fukuda, R.; Hasegawa, J.; Ishida, M.; Nakajima, T.; Honda, Y.; Kitao, O.; Nakai, H.; Vreven, T.; Montgomery, J. A., Jr.; Peralta, J. E.; Ogliaro, F.; Bearpark, M.; Heyd, J. J.; Brothers, E.; Kudin, K. N.; Staroverov, V. N.; Keith, T.; Kobayashi, R.; Normand, J.; Raghavachari, K.; Rendell, A.; Burant, J. C.; Iyengar, S. S.; Tomasi, J.; Cossi, M.; Rega, N.; Millam, J. M.; Klene, M.; Knox, J. E.; Cross, J. B.; Bakken, V.; Adamo, C.; Jaramillo, J.; Gomperts, R.; Stratmann, R. E.; Yazyev, O.; Austin, A. J.; Cammi, R.; Pomelli, C.; Ochterski, J. W.; Martin, R. L.; Morokuma, K.; Zakrzewski, V. G.; Voth, G. A.; Salvador, P.; Dannenberg, J. J.; Dapprich, S.; Daniels, A. D.; Farkas, O.; Foresman, J. B.; Ortiz, J. V.; Cioslowski, J.; Fox, D. J.; *Gaussian09*, revision D.01; Gaussian, Inc.: Wallingford, CT, 2013.
- (58) Yanai, T.; Tew, D. P.; Handy, N. C. *Chem. Phys. Lett.* **2004**, *393*, 51.
- (59) Hättig, C.; Weigend, F. *J. Chem. Phys.* **2000**, *113*, 5154.
- (60) Bannwarth, C.; Grimme, S. *J. Phys. Chem. A* **2015**, *119*, 3653.
- (61) Bannwarth, C.; Grimme, S. *Comput. Theor. Chem.* **2014**, *1040–1041*, 45.
- (62) Bruhn, T.; Schaumlöffel, A.; Hemberger, Y.; *SpecDis*, version 1.64; University of Würzburg: Würzburg, Germany, 2015.
- (63) Bringmann, G.; Bruhn, T.; Maksimenka, K.; Hemberger, Y. *Eur. J. Org. Chem.* **2009**, *2009*, 2717.
- (64) Ekström, U.; Visscher, L.; Bast, R.; Thorvaldsen, A. J.; Ruud, K. *J. Chem. Theory Comput.* **2010**, *6*, 1971.
- (65) Lin, Y.-S.; Li, G.-D.; Mao, S.-P.; Chai, J.-D. *J. Chem. Theory Comput.* **2013**, *9*, 263.
- (66) Lu, T.; Chen, F. *J. Comput. Chem.* **2012**, *33*, 580.
- (67) Humphrey, W.; Dalke, A.; Schulten, K. *J. Mol. Graphics* **1996**, *14*, 33.
- (68) Ishikawa, R.; Katoh, K.; Breedlove, B. K.; Yamashita, M. *Inorg. Chem.* **2012**, *51*, 9123.